

MICROCOPY RESOLUTION TEST CHART
NATIONAL BUREAU OF STANDARDS-1963-A

12

DNA 6152F

MODELING OF IMPLoded ANNULAR PLASMAS

John U. Guillory
Robert E. Terry
JAYCOR
205 South Whiting Street
Alexandria, Virginia 22304

1 April 1982

Final Report for Period 1 November 1980-1 November 1981

CONTRACT No. DNA 001-79-C-0189

APPROVED FOR PUBLIC RELEASE;
DISTRIBUTION UNLIMITED.

THIS WORK WAS SPONSORED BY THE DEFENSE NUCLEAR AGENCY
UNDER RDT&E RMSS CODE B323082406 T99QAXLA00020 H2590D.

Prepared for
Director
DEFENSE NUCLEAR AGENCY
Washington, DC 20305

DTIC
ELECTE
MAR 30 1983
S B

UNCLASSIFIED

SECURITY CLASSIFICATION OF THIS PAGE (When Data Entered)

REPORT DOCUMENTATION PAGE		READ INSTRUCTIONS BEFORE COMPLETING FORM
1. REPORT NUMBER DNA 6152F	2. GOVT ACCESSION NO. AD-A126179	3. RECIPIENT'S CATALOG NUMBER
4. TITLE (and Subtitle) MODELING OF IMPLoded ANNULAR PLASMAS		5. TYPE OF REPORT & PERIOD COVERED Final Report for Period 1 Nov 80 - 1 Nov 81
7. AUTHOR(s) John U. Guillory Robert E. Terry		6. PERFORMING ORG. REPORT NUMBER J207-82-009
9. PERFORMING ORGANIZATION NAME AND ADDRESS JAYCOR 205 South Whiting Street Alexandria, VA 22304		8. CONTRACT OR GRANT NUMBER(s) DNA 001-79-C-0189
11. CONTROLLING OFFICE NAME AND ADDRESS Director Defense Nuclear Agency Washington, DC 20305		10. PROGRAM ELEMENT, PROJECT, TASK AREA & WORK UNIT NUMBERS Subtask T99QAXLA000-20
14. MONITORING AGENCY NAME & ADDRESS (if different from Controlling Office)		12. REPORT DATE 1 April 1982
		13. NUMBER OF PAGES 42
		15. SECURITY CLASS. (of this report) UNCLASSIFIED
		15a. DECLASSIFICATION/DOWNGRADING SCHEDULE N/A since UNCLASSIFIED
16. DISTRIBUTION STATEMENT (of this Report) Approved for public release; distribution unlimited.		
17. DISTRIBUTION STATEMENT (of the abstract entered in Block 20, if different from Report)		
18. SUPPLEMENTARY NOTES This work was sponsored by the Defense Nuclear Agency under RDT&E RMSS Code B323082466 T99QAXLA00020 H2590D.		
19. KEY WORDS (Continue on reverse side if necessary and identify by block number) Radiation Plasma Z-pinch Generator Optimization 1-D MHD Code		
20. ABSTRACT (Continue on reverse side if necessary and identify by block number) During this period the primary emphasis has been on developing improved one-dimensional MHD code techniques for imploding plasmas with radiative energy flow, in diode electromagnetic cavities. Other computational tools necessary for this, including smooth interpolator routines, have also been developed for use in various parts of the NRL program modeling plasma radiation sources. These computational developments are summarized in Part A of this report and details are given in an accompanying technical report.		

DD FORM 1473
1 JAN 73EDITION OF 1 NOV 65 IS OBSOLETE
S/N 0102-LF-014-6601

UNCLASSIFIED

SECURITY CLASSIFICATION OF THIS PAGE (When Data Entered)

20. ABSTRACT (continued)

A secondary emphasis has been on developing simple approaches to the modeling of radiation, plasma dynamics, and generator optimization. We have developed simple, hopefully useful, tools in these areas, as described in Part B of this report, and their implementation is expected during 1982.

Lastly, we have during the contract period made a few suggestions for experiments, based on the projected possibility of doing some simple experiments on Gamble II. Our suggestions, aimed at studying processes likely to enhance K-line radiation power by various means, include an experiment to look at the voltage threshold for K-hot-spot emission and to look at the possibility of Al-Si radiations.



Accession For	
NTIS GRA&I	<input checked="" type="checkbox"/>
DTIC TAB	<input type="checkbox"/>
Unannounced	<input type="checkbox"/>
Justification	
By	
Distribution/	
Availability Codes	
Dist	Avail and/or Special
A	

RE: Classified References, Distribution Unlimited
No change in distribution statement per Ms. Melanie Bell, DNA/TIIM

CONTENTS

Page

A. One-dimensional MHD Code Techniques for Imploding Plasmas with Radiative Energy Flow	3
1. Motivation	3
2. 1D MHD Code: Computational Approach	8
3. Summary of Code Modules Developed.	16
4. Status of 1D MHD Code.	19
B. Simple Approaches to Models for Radiation, Dynamics, and Generator Optimization	20
1. Radiation Functions of Gaussian Cylinders.	20
2. Interlinked WIRES and SQUEEZE Codes.	22
3. Variational Approach to Optimizing Yield	25
4. Caveats to These Techniques.	29
C. Some Recommendations for Experiments	31
1. Qualitative Physics of Double Arrays	32
2. Observations on Beaded Discharges.	34
3. Potential Systems Impact	35
References	36

A. One-Dimensional and MHD Code Techniques for Imploding Plasmas with Radiative Energy Flow

1. Motivation

Existing models of imploding wire or puff gas plasmas^{1,2} leave a number of physical processes unexplored or only partially examined in their assessment of diode imploded plasmas as radiation sources. The one-dimensional implosion code to be described here is an attempt to increase the physical relevance of such models and to enhance the versatility and robustness of the numerical schemes used to implement them.

Our MHD computational efforts are aimed at improving the treatment of a number of processes over the MHD codes presently available. These include

- Photon-plasma energy exchange.
- Plasma thermoelectric radial stresses - how is the interior of the annular plasma pushed by the $J \times B$ forces on the outer surface?
- Current and field diffusion into the plasma "skin" - is the current penetration anomalously rapid as in classical pinch experiments, and how does the current layer evolve, quantitatively. The details affect the extent to which non-classical corona currents reduce the force on the bulk of the plasma.
- The fractions of electromagnetic power absorbed and reflected by the moving plasma load in the diode cavity. This is a central question since it measures the coupling efficiency of the hydrodynamic driver. Can the experimental diode waveforms be correlated to the plasma motion?
- The dynamic energy partition between electron thermal energy and ionization potential.

These considerations can be organized into several concrete goals for the calculation.

- 1) Find how important are the details of photon/plasma energy exchange in structuring the implosion trajectory and (spatially resolved) energetics. The transitions in qualitative characteristics (ranging from refrigerative collapse to strong reflection) noted in the core-corona model³ were quite sensitive to the opacity calculation. In a full 1-D implosion calculation the resolution of the enhanced "thermal conduction" due to direct photon/plasma energy exchange will provide a more accurate picture of the plasma emission profile.
- 2) Determine the role of separate ion and electron temperatures in establishing this emission profile and in governing the plasma dynamics. As compared with a single-temperature picture, one expects the proper two-temperature treatment to alter the pressure gradients in low density regions and change the opacity in higher density regions, perhaps altering the spectral mix of line and continuum radiation.
- 3) Examine the effect of the chemical potential (properly included in the plasma energy balance as a function of electron energy and ion density) on the implosion energetics and the emission profile.⁴ An accurate partition of incoming energy will probably provide lower (more physical) temperatures at peak implosion than earlier models.
- 4) Develop an accurate picture of the current penetration mechanisms. Diffusive transport of $E_z(r, t)$ (or B_θ) is dominant to a first approximation, but overall implosion performance is sensitive to the effective skin depth.⁵ The role of the free wave field components

in setting this skin depth has not been examined, and the rate of inward propagation for the drift-speed limitations in J_z may be affected by these components.

5) Resolve the sources of reflected power within the plasma load and relate them to the available measured waveforms from experiment. An electromagnetic calculation of all fields within the plane parallel diode opens one more channel of diagnostic information, and may provide a means of inferring plasma motion from measured waveforms. It will also provide a more accurate statement of energy conservation because the energy contained in the net free wave component will be included.

6) Examine the effect of radial ambipolar electric fields, and the resulting stress, on the implosion dynamics, particularly in the low density regions where drift speed limits are expected. The radial electric fields arise from thermoelectric effects and axial drifts of charge carriers. Large temperature gradients, allowed by weak cross field thermal conduction and enhanced ohmic heating in the corona plasma, may provide a significant radial electric field and resulting inward stress on the plasma.

Once these physical questions are addressed coherently, a smooth upgrading in the sophistication of the radiation emission and transport model becomes a fruitful exercise. With the radiative, hydrodynamic, and electrodynamic models structured from first principles there are no "free knobs" and the subsequent benchmarks with an appropriately configured experiment, if successful, provide a firm basis for similar theory in more difficult and perhaps more practical diode configurations.

Apart from these physical questions are various topics arising in the numerical implementation of whatever implosion model is selected. First is the choice of grid; a typical simulation will show the model plasma compressed several orders of magnitude during the course of a calculation. A strict Eulerian fluid calculation can thus lose its spatial resolution at the final collapse, when this resolution is most needed. Moreover large density gradients are commonplace, and it is probable that the dynamics of the low density region are dominated by the balance of density gradients and magnetostrictive stresses. A Lagrangian description is thus preferable in an implosion/explosion calculation, so long as the external stresses on the system can be defined readily over the spatial domain of interest. On the other hand the equations governing the field (E_z) generating the implosion are solved most naturally in the fixed laboratory frame. The electromagnetic problem therefore requires an interpolation capability which can map external stresses onto a convecting fluid and extract field sources from this moving fluid. The natural compromise adopted here is a completely Lagrangian fluid model convecting through a laboratory-frame (Eulerian) electromagnetic grid. The electromagnetic grid can be made sufficiently non-uniform to concentrate the E_z information density near the axis while the smoothly distorted Lagrangian fluid grid is a natural choice for an accurate resolution of density gradients.

The second numerical topic is the choice of E_z or B_θ as the fundamental electrodynamic variable. In our view the more convenient selection is E_z because it is the natural field from which to establish drift-speed limitations on the current density. Using B_θ and $J_z = \frac{c}{4\pi} (\nabla \times B_\theta)_z$ in a drift speed limitation algorithm has two disadvantages: the current is derived from a potentially noisy differentiation process, and the limit $J_z = en_e c_s$ does not

imply a completely local value for E_z because the conductivity depends on B_θ , and hence on J_z at other grid points. It is clearly possible to remove the second problem by iteration, but the physical process providing the drift speed limit is a local (fine scale) one. Proceeding first from the local values of E_z , then iteratively establishing small corrections to the (possibly limited) J_z from non-local considerations, is a more natural way to impose the limit and is probably less noisy.

A third point is the selection of forward time integration methods. A common preference for conservatively advanced explicit integrators must be examined carefully in the context of this radiatively coupled problem. As the level of sophistication in the radiative transfer physics is increased a considerable expense is incurred for each fluid time derivative. This expense will scale linearly with the number of frequency domains and quadratically with the spatial resolution. In order to optimize the complete algorithm it is therefore necessary to make the best possible use of every time derivative available from the space-time mesh. Moreover, as distinct from calculations dominated by processes internal to the fluid, the problem of simulating an electromagnetically driven implosion requires a self-consistent time evolution of both field and fluid. This class of problems is more likely to be handled efficiently and accurately by an implicit method, or at least by a predictor/corrector scheme. This choice has only the disadvantage of being more cumbersome to implement, and, as described below, the methods chosen make a smooth transition from "nearly explicit" to "fully implicit." As dictated by the performance characteristics of the complete algorithm, the user will be able to optimize the accuracy and cost tradeoff by several means.

A final consideration is the accuracy of spatial differentiation within either the hydrodynamic or electrodynamic algorithms. If these algorithms can make good use of non-uniform meshes in space and time, then one can sustain useful accuracy with fewer points. The common differentiation methods based on finite differences are quite accurate when a dense mesh is admissible, but if one wishes to keep down the cost of radiative transfer calculations a higher order, smoother scheme is preferable. Some useful alternatives are discussed in Section A.3.b. We have developed such schemes, involving smooth interpolators, as one segment of our computational effort, and this has already shown its utility in interfacing various parts of the NRL radiation physics with our plasmadynamic codes.

2. 1D MHD Code: Computational Approach

The specific physical content of the model has been described elsewhere.^{6,7} The task of implementation can be readily broken down into the three problem areas treated below - electromagnetics, hydrodynamics, and radiative transfer. The requirements for each problem area and a summary of the algorithms employed are given.

The electrodynamic problem statement is simple: given voltage waveforms at the periphery of the diode, establish the E and B fields everywhere in the interior for the duration of the implosion process. By driving the diode E/M model at one radius with a voltage waveform, the current drawn by the load and the voltage waveforms at any interior point are available as predicted observables/diagnostics of the code and the experiment.

Conventional approaches replace the vacuum portion of the diode with a circuit relation derived from Faraday's law, but a complete electromagnetic calculation provides more information. If this latter goal is chosen then the issue of efficient and effective calculation becomes an important question. With the implosion model discussed here the choice has been to admit either option, the full electromagnetic computation or the diffusive limit and circuit equation.

For the first option, it is instructive and in many ways practical to utilize the generalized Hertz vector potential. First, this new potential reduces the electrodynamics to a single component of a single vector wave equation. This reduction simplifies the calculation by placing no self-consistency constraints on the time evolution of the fields E_z , B_θ . The required self-consistency is automatic when E_z , B_θ are derived from a single potential Z_z . Second, the coupling term between field and plasma is properly defined to all orders in the radial fluid convection velocity and smoothly admits marginally stable drift-speed limited conduction and (quasi-static) thermo-electric contributions. Properly, as fast time scale phenomena which track the instantaneous state of the system, these effects should be calculated from a single time slice of information. Without the Hertz vector formulation, an electromagnetic calculation evolving E_z , B_θ separately can only accomplish this to the extent that it satisfies the temporal self-consistency constraint mentioned above. Third, the coupling term is a spatial convolution with a fixed Green's function. The spatial averaging will generally serve to lower the noise level of the calculation by damping any chatter that may appear on the discrete source array extracted from the plasma representation. Fourth, while the use of Z does require the

extraction of high order spatial derivatives from discrete data to form the E and B fields and the sources for the Z equation, the accuracy of such spatial differencing can be improved by the use of so-called smooth interpolators.⁸ The estimation of local E_z fields from the parent Hertz vector by means of these splines is routinely accurate to $[10^{-6}]$, even between the input data points.

The Hertz-vector-based electromagnetic calculation proceeds from a spatially discrete set of information $\{Z, \partial_T Z, J, \partial_T J, \partial_T^2 J\}$, given at a single time. The first two elements of this set are defined at fixed radial points; the last three, established (sequentially) on a convecting (Lagrangian) grid of plasma cell centers. The local values of E, B at any such time level are determined by $(Z, \partial_T Z, J)$ and partially determine the plasma stress and heating rates. From the values of $\partial_T J, \partial_T^2 J$, a spatial convolution produces the Hertz vector source terms. These source terms are interpolated for use in an explicit wave quadrature formula which advances the Hertz vector and its partial time derivative in order to establish $Z, \partial_T Z$ at any subcycle time step (used in the thermal conduction scheme) or at the next major time level.

The second electrodynamic option is that of E-field diffusion (which can be derived from the Hertz potential wave equation in the limit that incoming and outgoing waves are in detailed balance). This limit is approximate but reasonably accurate in the plasma where the conduction current exceeds the displacement current. It neglects the net displacement current, making any detailed outgoing wave calculation impossible because no wave source is extracted from the plasma. Reflected power is manifested solely as a diminished voltage on the plasma load and the energy delivered is simply $\int^t dt (I_{\text{plasma}} \cdot V_{\text{gen}})$. Here only the plasma current waveform is available as

diagnostic information, insofar as the voltage at the convecting plasma vacuum interface is not usually available from experiment. The major simplification is that Z need not be explicitly employed; it is sufficient to diffuse the E_z field and calculate the B_θ field in a (self-consistent) quasi-static manner. Diffusion of E_z rather than B_θ is preferable because the criteria for drift speed limitation stem most directly from the application of an "E-field-to-local-J" mapping.

Diffusion-based electrodynamics proceeds concurrently with subcycled thermal conduction. A circuit relation sets the time varying value of E_z at the outer boundary of the plasma, and the time slice information $\{E_{th}, E', B, \dot{B}, \dot{\sigma}, \sigma\}$ defined on the (convecting) plasma cell centers determines the material derivative of E_z . Here $E'_z = E + \beta_r \times B_\theta$ is the field in the convecting frame; E_{th} is the axial thermoelectric field, arising from radial pressure gradients. The new field E_z at the next time level is determined implicitly by the time sequence of material derivatives. The plasma mesh evolves in response to the stresses partially determined by the local values of E and B . In this mode of operation some iteration is required in obtaining both DE_z/Dt and B_θ , in contrast to the electromagnetic calculation. (B_θ requires iterative refinement due to the magnetic field dependence of the plasma conductivity.)

In either the electromagnetic or the diffusive mode, the imposition of drift-speed limited conduction is straightforward because the $E_z(r,t)$ profile is established a priori, before J_z is estimated. The rational basis for preference between the two modes can be derived only when the goals of item (4) above are reached and when the comparative computation costs of well-tuned subroutines are established.

The hydrodynamic problem is readily formulated (once E, B are considered given) in terms of well-known techniques. The primary challenge is to produce a quiet, relatively robust algorithm capable of concentrating the computational effort on the faster time scales of the problem, minimizing the number of expensive derivative evaluations required, and retaining spatial resolution of very highly compressed plasma loads.

In view of these requirements a Lagrangian formulation of the two-fluid transport equations for number density, flow velocity, and temperature has been implemented. There are several simplifications to the complete set of transport equations which are appropriate to the imploding diode plasma, but the hydrodynamic model is essentially that of Braginskii.⁹ In particular the radial flow field is assumed to be identical for ions and electrons, the electron density is assumed to be in quasineutral equilibrium with the ion density (allowing only small ambipolar charge separations), and the system of moment equations is closed with an ideal gas equation of state relating the pressure and temperature for each fluid. This reduces the fluid variables to $\{n_I, V_r, T_I, T_e, \alpha, \epsilon_I\}$ where α is the degree of ionization and ϵ_I the average ionization potential for the current α value. However T_e is not a very good thermodynamic variable because it is tightly coupled to α , and to ϵ_I . In order to follow the ionization dynamics efficiently, we let $\theta_e = T_e + \frac{2\epsilon_I}{3\alpha}$ and evolve θ_e instead. The approximation of the collisional radiative equilibrium (CRE) model¹⁰ is to assume a very rapid establishment of α and ϵ_I from (given) n_I and T_e . Hence the usual heating sources and sinks for T_e , when α is fixed, become (in effect) heating sources and sinks for θ_e in the context of CRE ionization dynamics. From a sufficiently accurate representation of $\alpha(\theta_e)$ and $\epsilon_I(\theta_e)$ preprocessed by the complete CRE model and smoothly inter-

polated, one may simply advance θ_e (the "grand canonical temperature") and compute T_e , β , ϵ_I and all other transport coefficients from the θ -value obtained at any timestep. This latter method is presently implemented. As is common practice in Lagrangian calculations, one may also remove the ion density from the set of evolved quantities by conserving the total number of ions in any cell, unless a rezoning is done, and calculating the density n_I from the time varying cell volume. Hence the irreducible set of fluid variables to be evolved is $\{V_r, T_I, \theta_e\}$, with the $r \equiv \int^t dt_1 V_r(t_1)$ defining the variable mesh positions to be used in computing the density n_I . For the choice of diffusive electrodynamics, this set is expanded to $\{E_z, V_r, T_I, \theta_e\}$ and the separate evolution of $\{Z, \partial_t Z\}$ through the Hertz vector wave equation is discarded.

The complete set of magnetized, β -dependent transport coefficients has been coded in a single subroutine, and those required for the simplest relevant problem are the axial electrical conductivity, the radial ion and electron thermal conductivities and the radial thermoelectric coefficient. The expansion of the model to include radial ambipolar electric fields, viscous stresses and viscous heating only requires activation of the axial thermoelectric and friction coefficients, and five viscosity coefficients. Moreover, because the relaxation time is the cornerstone of the transport calculation an extension into more strongly coupled plasma domains is quite straightforward on a cell-by-cell basis. The use of a modified relaxation time based on the local Coulomb logarithm is a useful first approximation in strongly coupled plasma transport¹¹ and can be relevant here in some simulations of wire or foil annular implosions.

The hydrodynamic calculation across a major time step proceeds from the $\{N_I, V_r, T_I, \theta_e\}$ at the beginning of the time step. Here N_I (the time invariant total number of cell ions), T_I and θ_e are defined at the cell centers, while V_r and $r(t)$ are defined at the cell interfaces. From this basic data the model calculates T_e, μ, ϵ_I , all transport coefficients, all heating rates and all fluid stress terms (after E and B have been established). The major time step is selected from a competition among the magnetosonic Courant condition, fractional cell area changes, local truncation error in estimating future accelerations (DV_r/Dt), and the most rapidly varying electromagnetic source terms. Once the major time step is set a time window is defined over which thermal conduction, compressional heating, radiative heating or cooling, and ion-electron exchange heating are subcycled at the cell centers (under an assumed cell boundary evolution). This subcycle is implemented using an (implicit) variable order Adams predictor-corrector or Gear method. At the completion of the subcycle the explicit flow field advance (and implied cell boundary motion) is either retained or iteratively refined (becoming the starting point for an implicit method). If desired the iteration proceeds until self-consistency is achieved. The self-consistency criterion is solution of the first order (non-linear) difference equation for the fluid acceleration, to a specified tolerance at all mesh points. For the diffusion based electrodynamics the subcycle includes the E_z field evolution as well.

A central element in the hydrodynamic model is the question of radiation transport. The algorithm presently implemented is a compromise between the full CRE calculation and the much simplified local approximation¹² of the SPLAT code. First, the emission function preprocessed by the

CRE model is represented over the relevant density and temperature domain. One such emission curve is required for each radiation category one wishes to calculate. A simple set of radiation categories is: {lines $h\nu < 1$ keV, lines $h\nu > 1$ keV, free-bound continuum, & Bremsstrahlung}. Next, for each radiation category a damping coefficient is computed for each cell.¹³ These damping coefficients are path integrated along a selected ray to produce a probability of escape for that photon category. From the escape probability field a matrix of coupling coefficients is derived. Once the coupling matrix is given, selected inner products with the vector of cell emissions for a particular category produce the cell-to-cell photon exchange and the net radiative loss to the plasma from any zone in each radiation category.

This formulation has the advantages of being easily expanded into a multiple group algorithm and easily modified to include other elements. At present Al and Ar are available, although the representation of θ_e is not yet available for Ar. The disadvantages lie in the added calculation of the coupling matrix and in the need to establish a fresh matrix for each radiation category. It is hoped that the use of implicit methods for the overall hydrodynamic advance will offset the cost of these radiative loss calculations by requiring fewer time derivative evaluations to achieve useful accuracy.

3. Summary of Code Modules Developed

a. The Imploding Plasma Radiator Code (Program ZDIPR)

A computer program is being constructed to solve the one-dimensional (in radius) time-dependent interaction of a plasma annulus (with temperature-dependent degree of ionization) and an electromagnetic driving field in a cylindrical cavity. It was shown previously that the number of equations describing the fields can be reduced and the computational stability probably improved by the use of a generalized Hertz vector, Z , from which E and B field vectors can be derived by differentiations. In the limit of high plasma density the wavelike term in the field equations can be neglected; this corresponds to a field-diffusion approximation. In simple cases — constant scalar conductivity for example — this gives the usual magnetic diffusion equation.

The program must couple field or Hertz potential quantities, evaluated most conveniently on a stationary (Eulerian) grid of points, with fluid equations describing the mass-motion (v) electron and ion temperatures (T_e, T_i), ionization (α), and effective conductivity (σ) of the plasma, all functions of r and t evaluated most conveniently on a Lagrangian, or co-moving grid. The differential equations are integrated forward in time by a variable-timestep method (GEAR), but because the plasma thermodynamic state evolves much more rapidly than the fields do, it is updated separately, on a fast timescale, with subcycle timesteps shorter than the major timestep T required for integration of the field and momentum equations. Doing these updates on different timescales is expected to save a significant amount of running time and expense in the computation, and may make the difference between a practical cost and an impractically large one.

In the code the subroutines that update the plasma state on the Lagrangian "r" mesh are MESHSTRESS (forces), TDOT (heating), CREOS (ionization state) and FLUIDOTS (material derivatives), all of these being used by the subroutine GEARBOX which controls the updating as part of the overall fluid-advance routine HYDROPUSH.

The subroutine that updates the field or Hertz potential variables on the Eulerian "R" mesh is called EPUSH or ZPUSH. When the Hertz potential representation is used, the subroutine HERTZDOTS updates the source terms in the potential equation at each major timestep. When the electric field diffusion representation is used, the corresponding subroutine EDOT updates the field source $\partial_t J$ and alternate plasma state movers (GEARBOX \rightarrow TETGEAR; FLUIDOTS \rightarrow TETDOTS) are used because different electromagnetic information is required.

This code, called ZDIPR, is now mostly written and some of its portions have been separately checked. Further testing and integration of the various subroutines will be carried on in the coming weeks.

b. The Smooth Interpolator Packages

Computer programs have been written (and are currently in use) which fit smooth spline functions to discrete data. The smooth functions are sums of Gaussians, error functions, or integrals of the error function, at the user's option. The user specifies a typical width parameter, and the smoothness of the representing functions depends on the width parameter chosen (iteration of the choice of width may be necessary). When optimized, the fitting functions also have smooth first and second derivatives (to within 6 significant figures in a typical example). These programs - REPIT which represents the data by spline functions (using subroutine SMILAM), and

CHECKIT, which evaluates the interpolant over any specified domain, are described more fully, along with the underlying theory, in Chapter II of the accompanying Technical Report (JAYCOR Tech. Report J207-82-002). These user-oriented programs are of great importance in the plasma-radiation and plasma dynamics community, and have been made available to users working in these areas at NRL. They are a necessity in codes which are required to extract smooth fields from potentials given at discrete data points, including the ZDIPR code described in Section 3.a. above.

4. Status of 1D MHD Code

The HYDROPUSH ensemble of subroutines has been partially written; given a predetermined E-field, the time step choice STEPPER and the iteration of the mesh are coded. FLUIDOTS, which determines the material derivatives of velocity and temperature, has been coded; its companion for the diffusive code has been designed and is being coded. GEARBOX, which carries out the integration, has been coded. The Jacobian routines, which assist DGEAR in integrating the equations efficiently, are being designed.

The field solver ZPUSH has been coded and the capability of unraveling E and B from the generalized Hertz potential Z has been established. (EFIELD and BFIELD are the subroutines which do this.) The evolution of Z in time is accomplished by WAVEQUAD and six functions which determine the elements of the wave equation quadrature's integrand. The code WAVEQUAD has been partially written and is undergoing testing at this time. The coding of EDOTS, which couples the external circuit to the plasma "boundary" current, is beginning. These subroutines all rely on previously-developed and tested routines, e.g. CREOS, BRAGINSKY, TDOT, which evaluate the basic plasma and radiation quantities.

A broad spectrum of smooth interpolator routines, just described in Section A.3.b. and the accompanying technical report, has been built, reduced to practice, and put to use in the EFIELD and BFIELD routines.

B. Simple Models for Radiation, Dynamics, and Generator Optimization

The search for simple but approximate models capable of giving radiation scaling laws at low cost continues alongside the larger-scale computer modeling. To this end we have initiated three interrelated calculations:

- (1) radiation blanketing and energetics for cylinders with Gaussian ion density profiles.
- (2) generalizing the JAYCOR SQUEEZE code, which describes approximately the dynamics of the plasma and radiation after assembly onto the axis, and interlinking it with the SAI WIRES code, which describes primarily the run-in phase of the implosion prior to assembly. The results of calculation (1) are to be used in the equations.
- (3) a calculus-of-variations approach to deriving explicit equations or computational algorithms for the machine current or voltage pulse profiles and the plasma initial conditions that optimize the desired radiative loss. The results of calculations (1) and (2) are to be used in this one.

Each of these areas will be described briefly now to show their justification and interrelation as well as the mode of approach to them.

1. Radiation Functions for Gaussian Cylinders

An assembled radiating plasma cylinder, partly opaque to its own radiation, is described by a density profile $n_i(r)$ with typical radius R (say the radius at half-maximum of $1/e$ -maximum density), a central density $n_0 = n_i(0)$, and an electron temperature profile $T(r)$. If radiative heat transport were very fast, one could imagine $T(r)$ being uniform: $T(r) = T$

everywhere. In that oversimplified baseline case one can use the NRL radiative transport multicell code to calculate the total radiative energy loss rates, for photons with energy above and below energy E_c , i.e.

$$P^>(n_0, [n_i(r)], T), \quad P^<(n_0, [n_i(r)], T).$$

Because most interesting density profiles qualitatively appear Gaussian, we specialize in this baseline case to Gaussian $n_i(r)$, so that the radiative loss functions become

$$P^>(n_0, R, T), \quad P^<(n_0, R, T).$$

However, in reality, at the edges of such plasmas the radiative heat transport can never keep the plasma at the central temperature. Radiative heat loss insures that there will be a falloff of $T(r)$, i.e. a cooler blanket surrounding the hot region. This blanket generates radiation in the $P^<$ category, and absorbs radiation in the $P^>$ class, so it is important in both the diagnostics and the energetics. Even if the blanket layer is thin compared with the cylinder radius, its optical depth may be significant (as in the case of stars), because the local opacity increases as the temperature falls with r . There may also be a hotter tenuous corona outside the blanket, but the density is too low to be of importance in the radiation energetics.

So we are preparing to calculate with multicell techniques the corresponding self-consistent $T(r)$ and $P^<$ and $P^>$ for a Gaussian density profile (with uniform heat input maintaining $T(r)$ constant), and thus to characterize the width of the blanket $\delta R(n_0, R, T_0)$ formed by the temperature profile $T(r; n_0, R)$, as well as the new radiated powers

$$P^>(n_0, R, T_0) \text{ and } P^<(n_0, R, T_0),$$

where T_0 is the central temperature.

Simple analytic fits to these functions will then provide a useful tool in that they can be put into the energy equation, which together with the momentum equation and a circuit equation determines the radiation scaling of such a model assembled plasma. The momentum, energy, and circuit equations, in such a simple model, are three ordinary differential equations, and their computational solution is much simpler than the MHD fluid equations used for the more exact modeling. These simple equations and their method of solution are discussed next.

2. Interlinked WIRES and SQUEEZE Codes

In a combined JAYCOR/SAI/NRL effort characteristic of this program we have begun combining the SAI WIRES code (Mondelli, 1981)¹⁴ for the run-in phase of a multi-wire array implosion, with a generalization of the JAYCOR SQUEEZE code (Guillory, 1980)³ for the assembled plasma compression and radiation phase. The WIRES code model is followed until the imploded, thermally expanded wires just touch. The plasma is then smoothed to a thick annular layer, and continues the implosion in a manner akin to the JAYCOR SPLAT code until a non-hollow cylinder is formed. The SQUEEZE code then describes the dynamics of the assembled plasma, at least until several growth times for macroscopic fluid instabilities, whereupon the plasma no longer follows any simple one-dimensional theory.

The WIRES code, described more fully elsewhere,¹⁴ consists of a simple Newton's-law dynamical equation for the radial position of the N wires, a circuit equation relating the voltage, current, and time-

varying inductance of the array, and an equation for heating of the wires in the presence of blackbody radiative losses, with the size of individual wires swelling as they heat. When these cylinders touch, they are replaced by an annulus of plasma of the same total area, and this is further compressed onto the axis by the total current in such a way that the inner radius b moves at the finite speed $|\dot{b}| = |\dot{a}| + c_s$ (c_s the sound speed) and the outer radius a is governed by

$$m\ddot{a} = kI^2(t)/a + 2\pi a l (1 + Z(T)) nT,$$

with I the current, Z the degree of ionization, n the ion density, and T the temperature. This is the small-skin-depth limit of equation 4 in Ref. 3, i.e. the same as the SPLAT code.

The SQUEEZE code, originally written with built-in simple equations for Aluminum ionization, has been generalized, and takes over the modeling of dynamics once the inner radius of the annulus has shrunk to zero. This code consists of solving simultaneous ordinary differential equations for the radius and temperature of a radiating cylinder compressed by the force of a given current $I(t)$.

Splitting the second-order force equation for \ddot{r} into two first-order equations, we have:

$$\begin{aligned} \dot{r} &= v \\ \dot{v} &= [A Z_1(T) T - B] r^{-1} \\ \dot{T} &= \{[ACZ_1(T) T + BD] v/r - R(r, T)/r^2 + K_\Omega\} / Z_2(T) \end{aligned}$$

where A , B , C , D and K_Ω are constants in the simplest model (the current is

held constant in that model), $R(r, T)$ describes the temperature-dependence and apacity dependence of the radiative cooling. In the optically-thin limit R is a function of T only.

The functions $Z_1(T)$ and $Z_2(T)$ are related to the degree of ionization $\bar{Z}(T)$ by $Z_1(T) = \frac{3}{2}[1 + \bar{Z}(T)]$, describing the total number density of particles (ions and Z electrons per ion) with energy $\frac{3}{2} kT$, and $Z_2(T) = \partial \epsilon_i / \partial T + \frac{3}{2} [1 + \bar{Z}(T) + T \partial \bar{Z} / \partial T]$, relating to the partition of new energy into increasing temperature and ionization. $\epsilon_i(T)$ is the average potential energy invested per ion in stripping them to the degree implied by electron temperature T .

The \dot{v} equation comes simply from

$$m \ddot{r} = 2 \pi r \ell \left(P - \frac{B^2}{8\pi} \right) \quad \text{with } B = \frac{2I}{cr} \quad (\text{cgs units})$$

and with $P = (n_e + n_i) T = \frac{N_i}{\pi r^2 \ell} [1 + \bar{Z}(T)] T$.

The \dot{T} equation comes from

$$\frac{d}{dt} \left\{ \frac{3}{2} N_i (1 + \bar{Z}) T + N_i \epsilon_i \right\} = - \frac{d}{dt} \left(\frac{1}{4} m v^2 \right) + (P - B^2/8\pi) \frac{d}{dt} (\pi r^2 \ell) - P_{\text{rad}} + I \cdot E$$

where the mean kinetic energy

$$\frac{m}{2} \int_0^r v^2(r') 2 \pi r' dr' = \frac{1}{4} m v^2(r)$$

thermalizes at a rate $\frac{1}{2} m \dot{r} \ddot{r}$ with \ddot{r} given from the equation of motion, which makes this term just half the $(P - B^2/8\pi)dV$ work. The coefficient AC thus

relates to work done by thermal pressure and BD relates to work done by magnetic pressure. The Ohmic heating term K_{Ω} is proportional to the current (excluding any carried by tenuous outer plasma) and voltage (including inductive correction). The radiative cooling function $R(r, T)$ is related to the total radiated power P_{rad} by

$$R(r, T) = \frac{P_{\text{rad}}(r, T)}{n_i^2 \pi r^2 \ell} = \frac{\pi r^2 \ell}{N_i^2} P_{\text{rad}}(r, T).$$

In the optically thin limit this is a function of T only; in the black-body limit it is proportional to $r^3 T^4$. The more general form of R in the code is to be got by fits to the MULTICELL computational results. In spite of the assumption of uniform density across the cylinder for dynamical purposes, it is probably a better approximation in the energetics to use radiative cooling results for Gaussian-density cylinders. Likewise the functions \bar{Z} and $\partial \epsilon_i / \partial T$ are calculated from smooth-interpolator fits to computational results, and are the same functions as used in the more sophisticated codes.⁵

The set of equations is easily generalized by adding a circuit equation to describe the current in terms of the voltage and the time-varying inductance and impedance of the plasma, but the resistive impedance depends on details of the field penetration which are not known a priori. Since during the short assembled "squeeze" phase the current does not change by a large percentage, we have chosen to take it as an empirical constant.

3. Variational Approach to Optimizing Yield

The problem of optimizing the time-integrated radiation above some critical photon energy E_c is, like other optimization problems, basically a calculus-of-variations problem. In the simple model of a uniform or a

Gaussian-profile cylinder radiator, there are, for any given material, four "coordinates" satisfying coupled first-order ordinary differential equations:

$$\begin{aligned} y_1(t) &= r, \text{ the cylinder radius} \\ y_2(t) &= v, \text{ the surface velocity} \\ y_3(t) &= T, \text{ the central temperature} \\ y_4(t) &= I, \text{ the current} \end{aligned}$$

In the energy-balance equation for T (the plasma is assumed dense enough that $T_e \sim T_i$) the radiated power, $P^>$ and $P^<$, above and below photon energy E_c , appears as a pair of functions of n , r , and T . Conservation of mass allows us to write $n(r)$ trivially from initial conditions, and thus the power radiated can be expressed as the known functional forms $P^<(r, T)$ and $P^>(r, T)$.

The object of the variational calculation is to maximize

$$\gamma^> \equiv \int_{t_1}^{t_{\text{End}}} dt P^>(r, T)$$

subject to the nonholonomic constraints on r , T imposed by the "constraint equations"

$$\begin{aligned} \dot{r} &= f_1(v) = v \\ \dot{v} &= f_2(r, v, T, I) \\ \dot{T} &= f_3(r, v, T, I) \\ \dot{I} &= f_4(r, v, T, I, V) \end{aligned}$$

i.e. $\dot{y}_n = f_n(y_1 \dots y_4, y_5)$, for $n = 1 \dots 4$. Here the independent "coordinate"

$y_5 = V(t)$ and the initial conditions are varied in order to achieve the maximum $Y^>$. $V(t)$ represents the applied voltage history.

The functions $P^<(r, T)$ and $P^>(r, T)$ correspond to functions suggested for computational evaluation in Section 1. It is expected that they can be fit by relatively simple algebraic forms. The integral $Y^>$ is maximized by introducing 4 Lagrange multiplier functions $\lambda_n(t)$ and solving the eight differential equations

$$\dot{\lambda}_n = - \sum_{m=1}^4 \lambda_m \frac{\partial f_m}{\partial y_n} - \frac{\partial P^>}{\partial y_n}$$

$$\dot{y}_n = f_n (y_1 \dots y_5).$$

The control function $y_5(t)$ is then determined by the algebraic relation¹⁵

$$\lambda_2 \frac{\partial f_2}{\partial y_5} + \lambda_3 \frac{\partial f_3}{\partial y_5} + \lambda_4 \frac{\partial f_4}{\partial y_5} = 0.$$

There is the complexity of a change of constraints at the time t_m when the wires merge into an annulus, and at the time t_1 when the annulus assembles into a cylinder. One may specialize this variational technique to the assembled cylinder, where the trajectory equations are those of the generalized SQUEEZE code, with the inclusion, hopefully, of realistic functions $P^>(r, t)$ and $P^<(r, T)$ fit from the proposed computer evaluation for Gaussian cylinders. Here, to keep the system of equations simple, we may to a first approximation eliminate the circuit equation $\dot{y}_4 = f_4 (y_1 \dots y_5)$ after the time t_1 , observing that the current does not change by a large percentage during the short-lived assembled phase of the discharge, where the radiation is important.

But one must then couple this $t > t_1$ dynamics to the $t < t_1$ dynamics.

The variational problem, with the lower integration limit on $\int P^> dt$ set equal to t_1 , then formally provides an optimization of this quantity by varying the current and the "initial" conditions r_1, v_1, T_1 at the beginning of the assembly (t_1). Since these ordinary differential equations can be solved computationally much more easily than the MHD equations, and since they are designed to lead to optimization equations rather than dynamic information, it is hoped that they can play a valuable role in system design at low cost, in spite of their very approximate nature.

4. Caveats to These Methods

The radiative output of a Gaussian-density cylinder is partially controlled by the temperature of the outer, cooler blanket. The radial energy-flow equation must contain a radially-dependent heat source to give a quasi-steady radiation rate and T_e profile. To the extent self-similar compressional heating provides the heat source, one can take the source to be uniform, i.e. position-independent. But Ohmic heating, which is expected to supply a smaller fraction of the energy, occurs primarily near the edges, and to the extent that it is important, it heats predominantly the blanket region, reducing its opacity. The radiation outputs are thus shifted toward those for the isothermal profile at the same central temperature. This puts the actual radiation picture somewhere between the isothermal and the blanketed results calculated. The sensitivity to such edge heating can be easily evaluated.

Also, the heating and radiation are not in balance for a real time-dependent system. The assumption of approximate balance to give a radiation output above and below photon energy ϵ_c is justified only insofar as the temperature profiles are similar in the dynamic and the steady problems.

The caveats of the combined WIRES/SQUEEZE calculation are primarily in the model equations and in the zero-dimensional nature (i.e. radial structure, including time-varying blanketing effect, is not resolved). One can see the latter caveat as follows: imagine two different systems of collapsing annular plasmas, one with a sharp leading edge (i.e. steep density gradient on the inner edge) and the other with a soft leading edge and a steep trailing edge. When the first plasma assembles its kinetic energy is 'thermalized' more rapidly, pushing the radiation tradeoff toward a shorter pulse at higher temperature, while the slower implosion may radiate longer, remaining cooler. A spatially resolved MHD code can discriminate between

these implosions, while the more approximate treatment has no consistent or reliable way to do so. Nonetheless, its low cost makes it potentially quite useful as a device for obtaining scaling with those variables which it can quantify.

It is simple to replace the WIRES run-in subroutine with one describing an annular gas puff. It is also simple to replace the run-in radiation/pressure-balance heating module used in WIRES with an alternative description of the thickness/temperature relation for the annular plasma. The obvious question is the sensitivity of results to these models, which is unknown as yet but can be evaluated from runs with the alternate model equations.

Finally, the caveats of the calculus-of-variations approach to voltage pulse shaping and choice of initial conditions are that such sets of equations often do not have unique solutions, or have no reasonable solutions without further constraint on the properties of the voltage pulse. The absence of uniqueness, if it occurs, is not serious. If there are several equally good solutions one simply picks the one that is technologically easiest. The absence of reasonable solutions, if this occurs, can force one to complicate the calculation by additional constraints.

The variational approach, because it uses the models of calculations (1) and (2), also suffers from their potential drawbacks; nonetheless, it is a significant step forward at relatively low cost, and we do not expect these drawbacks to be determining factors in system design.

C. Some Recommendations for Experiments

During 1981 JAYCOR also suggested experiments, at the request of NRL, which could be done on present devices and which might explore techniques for producing energetic radiation nonthermally where the plasma bulk temperature cannot be raised enough to emit such radiation thermally.

Two experiments were proposed on diode-imploded high-z plasma loads. The first involves implosion of an array of low-mass silicon wires onto an aluminum wire, and implosion of an outer array of silicon wires with an inner array of aluminum. The objectives of this experiment would be to observe radiation or any enhancement by the atomic and radiation physics specific to these two materials,¹⁶ to compare the radiation with and without a central wire,¹⁷ and to use the observed implosion time and diode current and voltage traces to infer the degree of magnetic shielding of inner conductors by outer ones, on the voltage pulse timescale.

The second experiment involves varying the charging voltage applied to a conventional low-mass array of high-z wires to observe and study the threshold-like onset of hard x-ray (10-100 keV) radiation from small dense regions of the final pinched discharge, as observed by x-ray pinhole photography.¹⁸ A first objective here would be to correlate the voltage at which this threshold occurs with the theory of modified-two-stream unstable regions of low density in series with higher density beads.¹⁹ The theory predicts that if the sausage instability reduces the density in the necked-off regions sufficiently, enhanced hard radiation will be produced as electrons heated in the low-density "beads". A second objective of this experiment is to determine whether this phenomenon can be used, as predicted, to tailor the "hard" component of the spectrum and make significant radiation production in the 10-100 keV range from discharges too massive or too high in Z to reach the temperatures needed for significant thermal K-line radiation.

1. Qualitative Physics of Double Arrays

Implosions of an annular array of silicon fibers onto an aluminum center wire, or of a large-radius silicon array and a smaller aluminum array on the axis, appear interesting. The atomic and radiative interactions of the silicon and aluminum at high temperatures have been treated in a 1981 report.¹⁶ Considerations here are that the temperatures of the Si and Al components must become more or less comparable at the same time. Although physical proximity of the two materials is not explicitly required, the requisite temperatures (~ 100 eV) are created only during the peak compression on axis, so that for practical purposes the more interesting and efficient radiation process can come about only when the load collapses onto the axial wire, or when the two loads coincide on axis. Separate arrays of different mass will tend to implode at different rates, corrected somewhat by magnetic shielding of the inner load by the outer one, so that the implosion timescale will tend to be that of the slower load.

While an annular outer conductor shields the applied electromagnetic field from an array of conductors inside it, this is not necessarily true if the outer conductor is a small number of wires distributed in annular fashion. To the extent that the electromagnetic pulse is not transmitted to the inner array, the time-history of such double array implosion with staggered wires would be expected to look like Fig. 1, in which the outer array implodes past the inner one but loses its $J \times B$ driving force in so doing, while the second array accelerates from rest. By suitable choice of the array masses and radii, the two implosions can be made to coincide on reaching the axis.

When the magnetic shielding is poor, the inner array is subject to some $J \times B$ force before being overtaken, and the timing of the two implosions

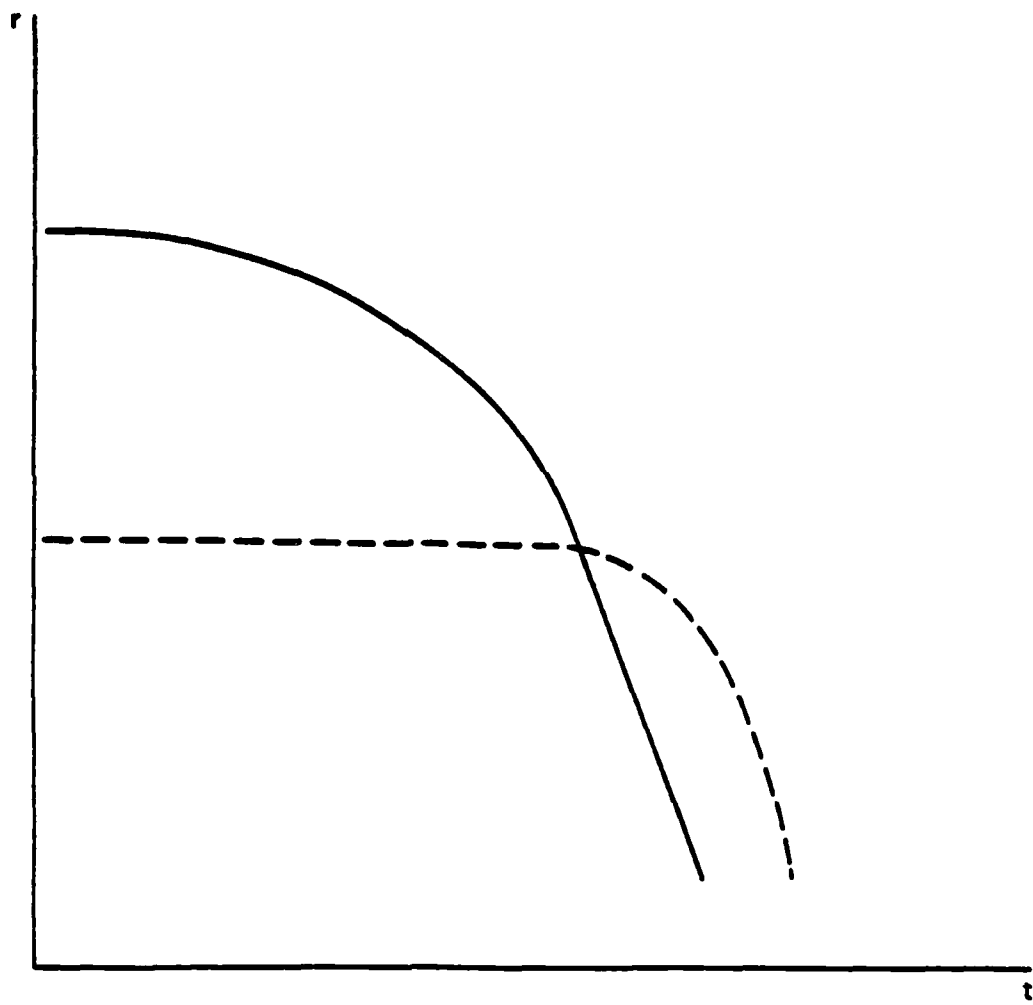


Figure 1. Radii vs. time, for an interpenetrating double array of wires.

is altered. This provides a potentially sensitive diagnostic for the distribution of $J \times B$ forces in such arrays, and should shed light on the degree of electromagnetic shielding (and hence the coupling efficiency) in the conventional annular wire arrays.

2. Observations on Beaded Discharges

There is a reasonable amount of evidence showing that at high voltages, exploding wires of high atomic number exhibit beading, including millimeter-size blobs of dense plasma as seen in the thermal radiation spectrum, and smaller hot spots of energetic x-ray emission. These discharges are unstable to sausage instability, and it is reasonable to expect the observed behavior. Imploded annular arrays of wires exhibit a more complex variety of inhomogeneities, including beading and helical distortions, reflecting the fact that they are unstable to corkscrew-like modes in addition to the $m=0$ sausage. It has been proposed¹⁹ that these inhomogeneities can be useful in allowing intense radiation by heating electrons strongly in the low-density regions and bringing about the energy deposition at the surface, or in the volume, of the denser beads.

While the beading is a quite chaotic process, certain conditions on voltage and minimum density on axis are predicted to give rise to such strong electron heating. This phenomenon has not yet been explored experimentally except in single wire loads¹⁸ and then no attempt was made to study the scaling of the hard radiation with voltage or to estimate densities in the less dense regions.

3. Potential Systems Impact of the Experiments

The simulation community is presently not able to build a device with the required combination of total radiated power, spectrum, and timescale for DNA objectives. The importance of making high-z diode-imploded plasmas radiate nonthermally in the K-line and Bremsstrahlung continuum is that insufficient energy is available with present-generation devices to make them radiate in this spectral range thermally, unless unreasonably low-mass arrays are envisioned. Two nonthermal processes, discussed in reports but not yet explored experimentally, hold some hope for enhancing the radiation from plasma sources to suitable levels. The experiments proposed were designed as preliminary looks at those two processes, and in passing provide important information about the electrodynamics and atomic physics of ongoing experiments.

References

1. R. E. Terry and J. Guillory, Development and Exploration of the Core/ Corona Model of Imploding Plasma Loads, JAYCOR report number TFD-200-80-001-DFR, 1980.
2. D. G. Colombant, M. Lampe and H. W. Bloomberg WHYRAC, A New Modular One-Dimensional Exploding Wire Code, NRL Memo Report 3726, 1978.
3. R. E. Terry and J. Guillory, Development and Exploration of the Core/ Corona Model of Imploding Plasma Loads, JAYCOR report number TPD-200-80-001-FR, p, 92.
4. *ibid* p. 44 and 45, pp 95-98.
5. R. E. Terry and J. Guillory, Annual Report on Modeling of Imploding Annular Loads, JAYCOR report number J207-81-004, 1981, p. 20.
6. *ibid*, pp 26-58, and Appendix D
7. R. E. Terry, J. Guillory and D. Duston, Generalized Hertz Vector Potentials and Their Application to Diode Imploded Plasmas, Bull. APS, 26, No. 7, Sept. 1981.
8. A Talmi and G. Gilat, Journal of Computational Physics 23, p. 93, 1977.
9. S. I. Braginskii, in Reviews of Plasma Physics, ed. M. A. Leontovich (Consultants Bureau, NY 1965).
10. D. Duston and J. Davis, Phys. Rev. A 21, May 1980.
11. Y. T. Lee (private communication).
12. R. E. Terry and J. Guillory, Development and Exploration of the Core/ Corona Model of Imploding Plasma Loads, JAYCOR report number TPD-200-80-001-FR, 1980, p.70.

13. J. P. Apruzese, J. Quant. Spectrosc. Radiat. Transfer 25., p. 419, 1981.
14. A. Mondelli, "The WIRES Code - A Simple Model for Implosions" in J. Davis et al. NRL Memo report 4796, March 1982 (S-CNWDI).
15. M. M. Denn, Optimization by Variational Methods, McGraw Hill 1969, p. 100.
16. J. P. Apruzese, J. Davis, and K. G. Whitney, Plasma Conditions Required for Attainment of Maximum Gain in Resonantly Photo-Pumped Ne IX. NRL Memo Report 4618, Oct. 1981.
17. R. Pohl et al., Experiments on Multiple Wire Arrays. R & D Associates Tech. Report RDA-TR-113301-002, Aug. 1980 (S-CNWDI).
18. D. Mosher and S. Stephanakis et al., Ann. NY Acad. Sci. 251, 632 (1975).
19. J. Guillory, Electron Heating in Strongly Beaded High-Z Pinch Discharges at High Densities, JAYCOR Report Number J207-81-003, May 1981.

DISTRIBUTION LIST

DEPARTMENT OF DEFENSE

Assistant to the Secretary of Defense
Atomic Energy
ATTN: Military Applications
ATTN: Executive Assistant

Defense Intelligence Agency
ATTN: DT-1B, R. Rubenstein

Defense Nuclear Agency
ATTN: RAAE
ATTN: RAEV
ATTN: STNA
ATTN: RAEE
4 cy ATTN: TITL

Defense Technical Information Center
12 cy ATTN: DD

Field Command/DNA
Lawrence Livermore Lab
ATTN: FC-1

Field Command
Defense Nuclear Agency
ATTN: FCPR
ATTN: FCTT, G. Ganong
ATTN: FCTT
ATTN: FCTT, W. Summa

Under Secy of Def for Rsch & Engrg
ATTN: Strategic & Space Sys (OS)

DEPARTMENT OF THE ARMY

Harry Diamond Laboratories
ATTN: DELHD-NW-P
ATTN: DELHD-NW-RA
ATTN: DELHD-NW-RI
ATTN: DELHD-TA-L

U.S. Army Nuclear & Chemical Agency
ATTN: Library

U.S. Army Test and Evaluation Comd
ATTN: DRSTE-EL

U.S. Army Missile Command
ATTN: Documents Section

DEPARTMENT OF THE NAVY

Naval Research Laboratory
ATTN: Code 2000, J. Brown
ATTN: Code 4770, I. Vitokovitsky
ATTN: Code 4720, J. Davis
ATTN: Code 4780, S. Ossakow
ATTN: Code 4773, G. Cooperstein

Naval Surface Weapons Center
ATTN: Code R40
ATTN: Code F31
ATTN: Code F34

Naval Weapons Center
ATTN: Code 233

DEPARTMENT OF THE AIR FORCE

Air Force Weapons Laboratory
ATTN: SUL
ATTN: CA
ATTN: NTYC
ATTN: NT
ATTN: NTYP

Ballistic Missile Office
ATTN: ENSN
ATTN: SYDT

Research, Development, & Acq
ATTN: AFRDQI

Space Division
ATTN: XR

Space Division
ATTN: YEZ

Space Division
ATTN: YGJ

Space Division
ATTN: YKF

Space Division
ATTN: YKS, P. Stadler
ATTN: YKM

Space Division
ATTN: YNV

Space Division
ATTN: YO

Strategic Air Command
ATTN: INT, E. Jacobsen

DEPARTMENT OF ENERGY

Department of Energy
ATTN: Ofc of Inert Fusion, S. Kahalas
ATTN: Ofc of Inert Fusion, T. Godlove
ATTN: Ofc of Inert Fusion, C. Hilland

DEPARTMENT OF ENERGY CONTRACTORS

Lawrence Livermore National Lab
ATTN: Tech Info Dept Library
ATTN: L-545, J. Nuckolls
ATTN: L-47, L. Wouters
ATTN: L-153
ATTN: L-153, D. Meeker
ATTN: L-401, W. Pickles

Los Alamos National Laboratory
ATTN: MS222, J. Brownell

Sandia National Lab
ATTN: M. Clauser, Org 5241
ATTN: G. Kuswa, Org 5240
ATTN: G. Yonas
ATTN: 3141
ATTN: J. Powell
ATTN: D. Allen, Org 9336

OTHER GOVERNMENT AGENCY

Central Intelligence Agency
ATTN: OSWR/NED

DEPARTMENT OF DEFENSE CONTRACTORS

Advanced Research & Applications Corp
ATTN: R. Armistead

Aerospace Corp
ATTN: V. Josephson
ATTN: S. Bower
ATTN: Technical Information Services

BDM Corp
ATTN: Corporate Library

BDM Corp
ATTN: L. Hoeft

Boeing Co
ATTN: Aerospace Library

Dikewood
ATTN: Tech Lib for L. Davis

EG&G Wash Analytical Svcs Ctr, Inc
ATTN: Library

General Electric Co
ATTN: J. Peden
ATTN: H. O'Donnell

IRT Corp
ATTN: R. Mertz

JAYCOR
ATTN: E. Wenaas

JAYCOR
ATTN: R. Sullivan
ATTN: E. Alcaraz
4 cy ATTN: J. Guillory
4 cy ATTN: R. Terry

Kaman Sciences Corp
ATTN: S. Face

Kaman Tempo
ATTN: DASIAN

DEPARTMENT OF DEFENSE CONTRACTORS (Continued)

Maxwell Labs, Inc
ATTN: A. Kolb
ATTN: W. Clark
ATTN: A. Miller
ATTN: O. Cole

McDonnell Douglas Corp
ATTN: S. Schneider

Mission Research Corp
ATTN: C. Longmire
ATTN: W. Hart

Mission Research Corp
ATTN: B. Godfrey

Mission Research Corp
ATTN: B. Passenheim

Pacific-Sierra Research Corp
ATTN: H. Brode, Chairman SAGE
ATTN: L. Schlessinger

Physics International Co
ATTN: C. Gilman
ATTN: C. Stallings
ATTN: G. Frazier

R & D Associates
ATTN: A. Latter
ATTN: P. Haas

R & D Associates
ATTN: P. Turchi

S-CUBED
ATTN: A. Wilson

Science Applications, Inc
ATTN: K. Sites

TRW Electronics & Defense Sector
ATTN: Technical Information Center
ATTN: D. Clement

Lockheed Missiles & Space Co, Inc
ATTN: L. Chase

Lockheed Missiles & Space Co, Inc
ATTN: S. Taimuty, Dept 81-74/154

4-
DT